Materials Letters: X 5 (2020) 100029

Contents lists available at ScienceDirect

Materials Letters: X

journal homepage: www.elsevier.com/locate/mlblux

Scale up of microwave annealed $FA_{0.83}Cs_{0.17}PbI_{1.8}Br_{1.2}$ perovskite towards an industrial scale

João Mascarenhas *, M. Alexandra Barreiros, Maria João Brites

LNEG, I.P. Estrada do Paço do Lumiar 1649-038 Lisboa, Portugal

ARTICLE INFO

Article history:
Received 28 June 2019
Received in revised form 30 September 2019
Accepted 11 November 2019
Available online 13 November 2019

Keywords:
Scale-up
Perovskite
PSC
Microwave annealing

ABSTRACT

Perovskite solar cells (PSCs) efficiency has rapidly increased from the initial 3.8 to recent 24.2%. This high efficiency has attracted serious worldwide researchers and industry attention due to their low material cost, and simple solution-based fabrication process. However, fundamental studies on PSCs are usually produced through lab-scale actions and carried out on small-area devices ($\leq$1 cm^2). Here we present the advances of up-scaling using microwave (MW) annealing of perovskite films on large area specimens (~16 cm^2), looking forward the industrial-scale. Morphological, structural and optical characterization were performed to confirm the effectiveness of the scaled up MW annealing.

1. Introduction

From the initial (2009) power conversion efficiency (PCE) of 3.8% [1], recent PSC record stands on 25.2% [2], however, these records have been accomplished on relatively small active areas (0.1 cm^2 or 0.03 cm^2) [3]. For large-area PSCs devices (>1 cm^2), though such similar area cells have been reported as having PCE in excess of 20% [4], there are fundamental issues that need to be addressed: (i) controllable thin film growth and deposition, (ii) scalable and reproducible process, (iii) high stability and long lifetime, and (iv) low toxicity.

Various thin-film deposition technologies have been developed, to fabricate large-area perovskite films of high quality (good film uniformity, reduced surface roughness, low density of structural defects, such as pinholes, etc.), being promising techniques blade coating, spray coating, chemical vapor deposition, and inkjet printing [5]. A common step required for the majority of these deposition processes is the thermal annealing of the perovskite layer aiming to drive off any residual solvent from the precursor and/or to control both the macroscopic morphology and the crystalline domain size. [6–10].

In previous work [11], we demonstrated that MW annealing process is an efficient and ultrafast low-temperature fabrication method of compact, pinhole-free, and highly crystalline perovskite, being the improvement in crystallinity and enhancement in perovskite grain sizes achieved by optimization of MW output power and irradiation time.

Here we present the advances of up-scaling using microwave (MW) annealing of perovskite films on large area (~16 cm^2), being the effectiveness of the MW annealing process confirmed by morphological, structural and optical characterization.

2. Material and methods

Cesium iodide, Lead(II) bromide, Lead(II) iodide and Hydrobromic acid from Sigma-Aldrich, Hydriodic acid from Alfa Aesar. Perovskite and TiO_2 compact layers' preparation are detailed described in [11].

MW annealing was performed in a multimodal cavity MW Research Applications Inc. oven, 1 kW nominal power and 2.45 GHz magnetron, temperatures being measured by a platinum-shielded S-type thermocouple placed 2 mm above the specimens. Specimens annealed on a transparent-to-MW ceramic fiber, Fig. 1-a). MW power was 50 and 100 W, and the time needed to crystalize the ~16 cm^2 perovskite films, was approximately 4 and 2 min respectively.

Conventional annealing (CA), 185 °C–30 min, was performed in a conventional furnace for comparison sake.

Scanning electron microscopy (SEM) was performed on a Philips XL30 FEG equipment. X-ray diffraction (XRD) patterns were

* Corresponding author.
E-mail address: joao.mascarenhas@lneg.pt (J. Mascarenhas).

https://doi.org/10.1016/j.mlblux.2019.100029
2590-1508/

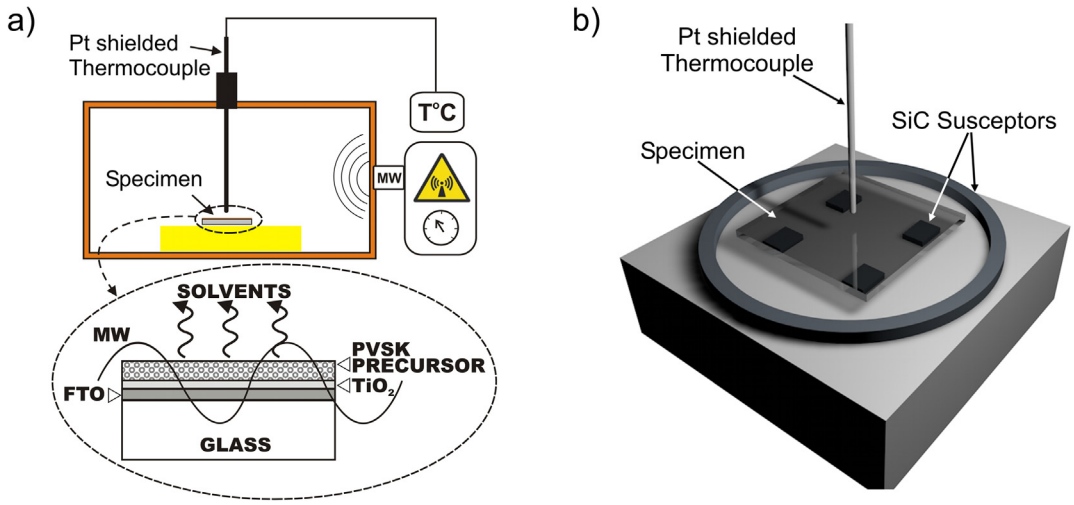

Fig. 1. a) MW oven set up; b) SiC susceptors arrangement.

recorded using a Panalytical MPD-XPert-Pro diffractometer in Bragg-Brentano configuration and Cu-Kα radiation source. Grain size and grain diameter average were determined by Digital Image Analysis in-house procedures based on SEM images taken with identical magnification from each specimen at different regions.

3. Results and discussion

Here we test the MW annealing process in large area specimens (16 cm^2) using formamidinium (FA) and cesium (Cs) mixed cation/iodide bromide mixed anion perovskite solution ($FA_{0.83}Cs_{0.17}PbI_{1.8}$-$Br_{1.2}$) [12] deposited by spin coating on a compact TiO_2 layer.

When irradiated by MW, sharp bared glass edges substrates experienced an inhomogeneous heating due to the so called edge effect [13], that occurs when MW diffract on the specimen's edge, rising locally the temperature, and consequently starting the crystallization on that site. To overcome this effect, we used aluminum thin sheet shield covering the FTO glass substrate's edges [14].

When the bared edges substrates were MW annealed, the crystallization starts on the near-edge region and continues towards the sample's center, as shown in Fig. 2a. The bared edges specimens, Fig. 2e), show perovskite decomposition near the edges, due to excessive temperature rise at these sites, the yellowish zones being PbI_2, as identified by XRD [11].

Contrarily, when specimens' edges were shielded with aluminum thin foil, Fig. 2f), crystallization path changed, the specimen's temperature rising being more effective in the specimen's center, which is natural in MW irradiated materials, Fig. 2c) [15]. Fig. 2f) shows the edge shielded specimen where the central dark zone is perovskite, and the contour not yet crystalized yellowish precursor. Longer times to transform this yellowish zone into perovskite result in decomposition of the central zone, already crystalized.

To avoid heterogeneities, one must ensure that the whole material is heated homogeneously. In fact, PSC's glass substrate, FTO and TiO_2, have their own contribution to MW heating. Glass is transparent to microwaves having no contribution to temperature rise [16]. FTO a non-stoichiometric semiconductor has high electrical conductivity, having a strong heating response [17]. TiO_2 shows moderate coupling to MW [16]. Finally, the perovskite precursor solvent DMF has a considerable large penetration depth compared to the film thickness (<1 μm) [18], what corresponds to uniform heating through the 1-dimension thickness of this material [19], contributing to the real heating of the active layer [20]. Hence, precursor material is effectively heated not only by its own coupling with MW, but also from the lower stack layers, mainly FTO [21].

So, the whole specimen being at the same temperature to allow a uniform precursor transformation is essential, Fig. 2d). Hence, in order to homogenize the specimen's temperature profile, an approach was made using SiC susceptors, Fig. 1b), which allowed crystallization of perovskite in the whole specimen, Fig. 2g). SiC susceptors, located near specimen corners, start to absorb MW energy from room temperature, and release heat radiation locally. As the specimens' center is already heated by MW, Fig. 2c), with this extra heating, a full material heating is attained, Fig. 2d).

Fig. 3 shows the perovskite microstructure of the conventional and MW annealed specimens and respective grain size distribution on the insets. CA perovskite shows a smaller grain size distribution when compared to MW annealed ones, Fig. 3a). Hence, the CA larger grain size population is in the range 2–3 μm with 48% share, Fig. 3a), whilst in all the MW annealed specimens (regardless MW power or with/without susceptors runs), the largest grain size population is in the range >12 μm, Fig. 3b), c) and d). As seen on the inset figures, larger grain size classes increase with MW power, being this at the expense of the immediately preceding ones, namely, larger grains grow at the expense of smaller ones (Ostwald ripening) [22]. As MW radiation produces both thermal and non-thermal effects on dielectric materials, being the MW annealing temperature lower compared to CA (80° versus 185 °C, respectively), it can be inferred that it is mainly the MW non-thermal effect that is responsible for this grain size increasing [11,23].

To assess the effectiveness of the MW annealing process in the whole specimens' area, we performed morphological, structural and optical characterization in different zones of the perovskite film area, Fig. 4. The perovskite film is compact and without pin holes all over the analyzed areas. Hence, in Fig. 4 it can be seen the grain size distribution across the 100 W, 80 °C MW annealed specimens, being the largest grains located at the central area. All XRD patterns show high intensity peaks, corresponding to the (1 0 0) and (2 0 0) reflections from cubic perovskite's characteristic planes, along in some sites with PbI_2 peaks, Fig. 4. In smaller grain size areas (3, 4, and 5), PbI_2 peaks can be attributed to a not completely crystalized precursor, whilst in the bigger grain size ones (1 and 2), its arising corresponds to an already decomposed perovskite.

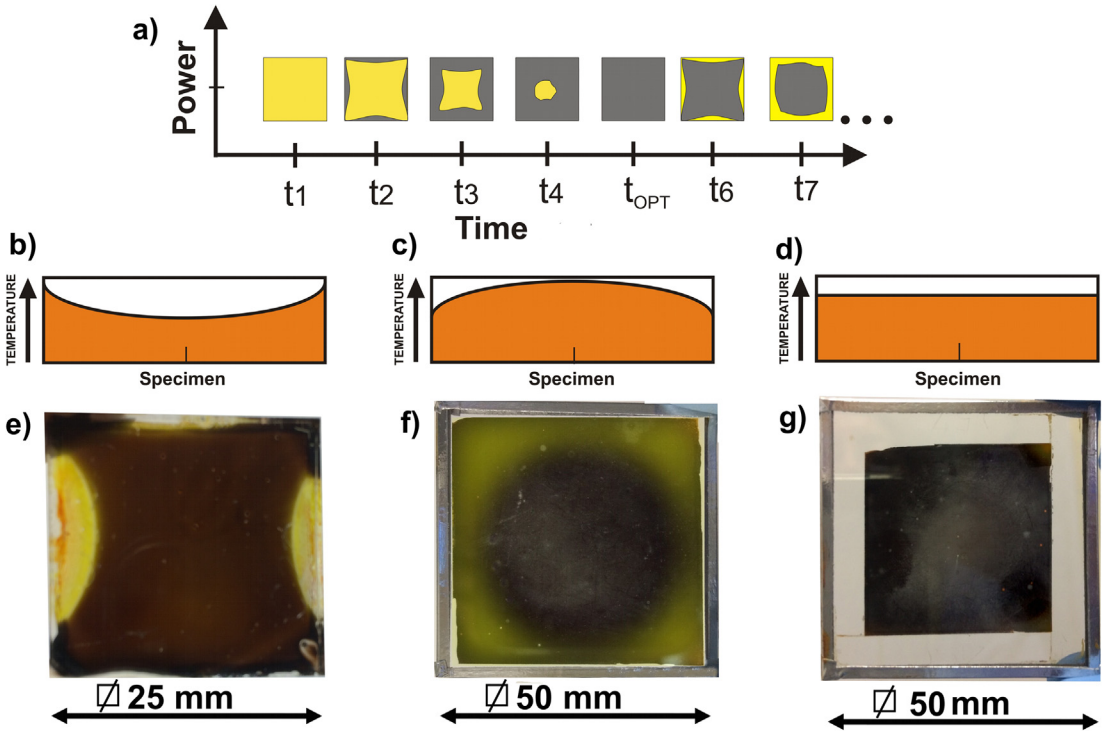

Fig. 2. MW perovskite crystalization evolution of bared/shielded edges glass specimens a) schematic crystallisation evolution with time for bared edges substrates; a), b) and e) Bared edges; c) and f) Al shielded edges; d) and g) Al shielded edges and susceptors.

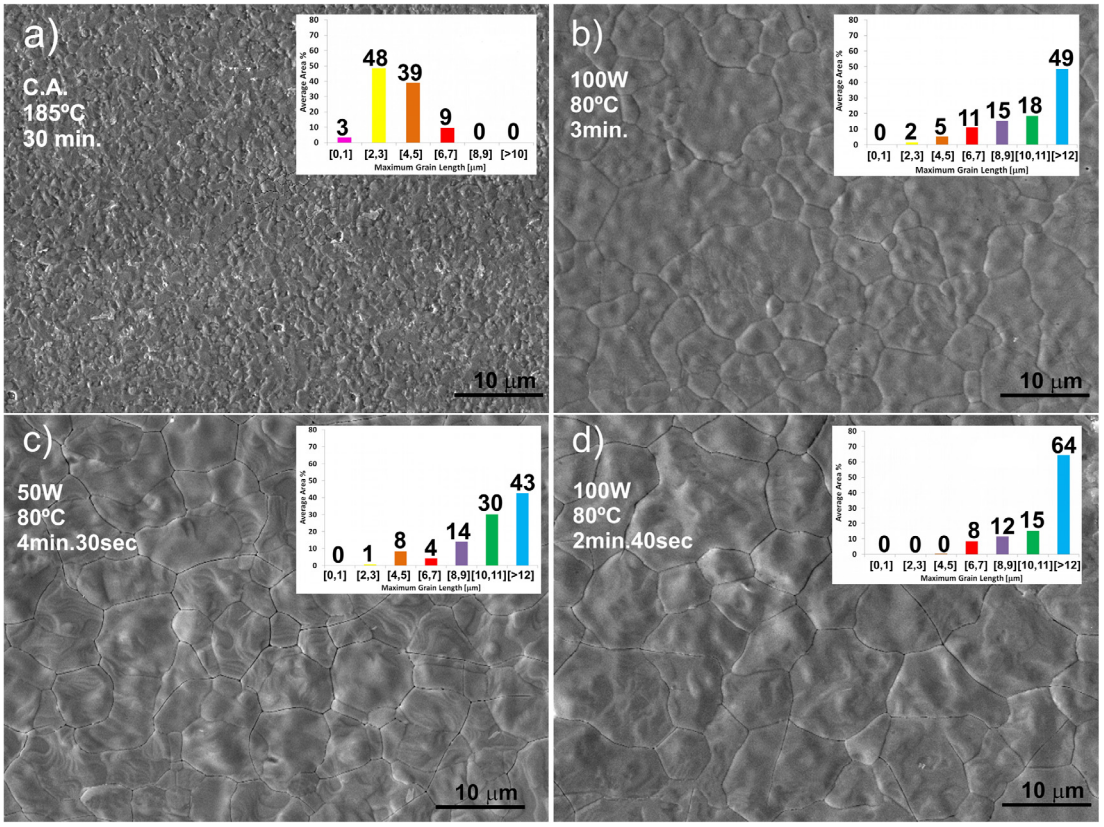

Fig. 3. Microstructures and average grain size distribution (insets) of $FA_{0.83}Cs_{0.17}PbI_{1.8}Br_{1.2}$ perovskites: a) Conventionally annealed; b) MW annealed; c) and d) MW annealed with susceptors.

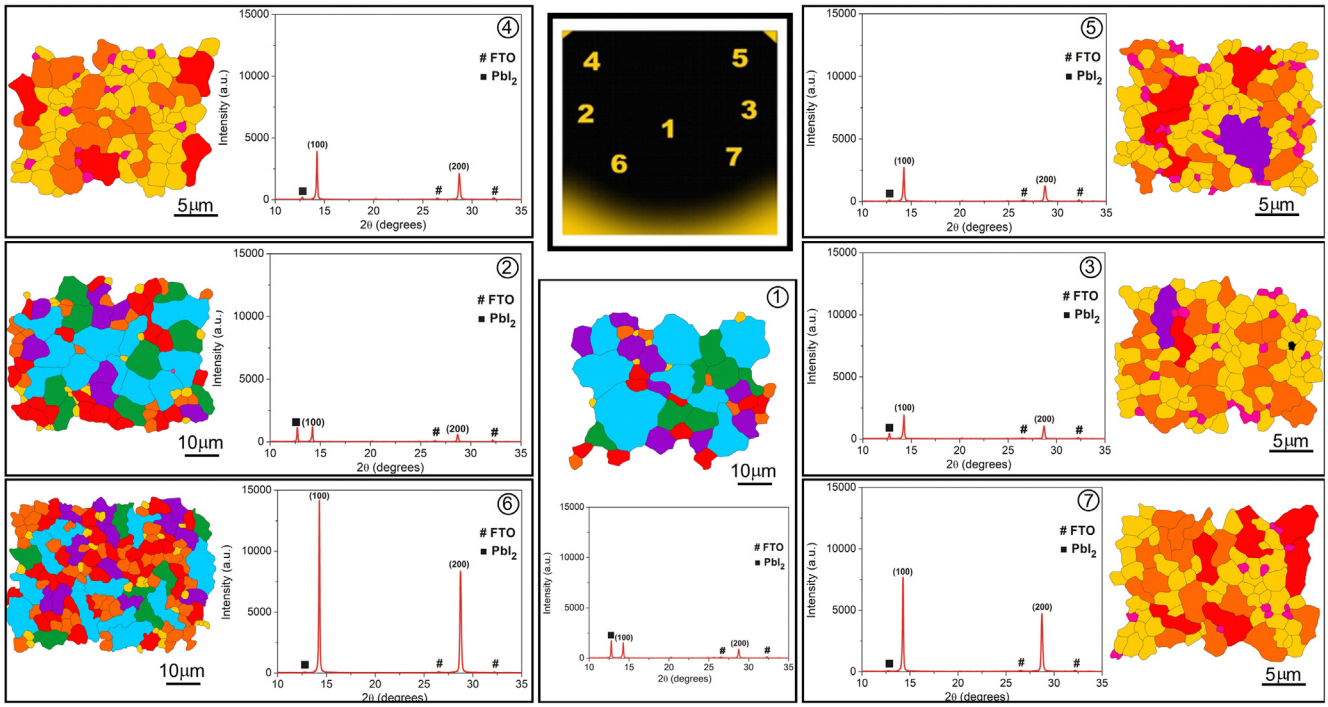

Fig. 4. $FA_{0.83}Cs_{0.17}PbI_{1.8}Br_{1.2}$ perovskite grain size distribution of 100 W/80 °C/3 min. (Al mask/without susceptors) annealed specimen and respective XRD patterns across it.

4. Conclusions

With this work, we proved the MW annealing efficiency to scale-up crystallized PSK films up to ~16 cm^2, at low temperature (80 °C) adjusting MW power and irradiation time, using SiC susceptors. These highly crystalline films (intense XRD peaks), have wide grain size (up to 12 μm), along with pinhole-free and smooth surfaces in all the analyzed areas, which is highly desirable for efficient perovskite solar cell fabrication.

Declaration of Competing Interest

The authors declare that they have no known competing financial interests or personal relationships that could have appeared to influence the work reported in this paper.

Acknowledgments

Work supported by National Funds through FCT-Foundation for Science and Technology under the projects AltaLuz (PTDC/CTM-ENE/5125/2014) and SuPerSolar (PTDC/NAN-OPT/28430/2017).

References

[1] A. Kojima et al., Organometal halide perovskites as visible-light sensitizers for photovoltaic cells, J. Am. Chem. Soc. 131 (2009) 6050.
[2] PV Efficiency Record Chart, https://www.nrel.gov/pv/assets/pdfs/best-research-cell-efficiencies.20190923.pdf (30/September/2019).
[3] Mengjin Yang et al., Square-centimeter solution-processed planar CH3NH3PbI3 perovskite solar cells with efficiency exceeding 15%, Adv. Mater. 27 (2015) 6363–6370.
[4] Yichuan Chen et al., Large-area perovskite solar cells – a review of recent progress and issues, RSC Adv. 8 (2018) 10489.
[5] Richard Swartwout et al., Scalable deposition methods for large-area production of perovskite thin films, Energy Environ Mater. 2 (2019) 119–145.
[6] Michael Saliba et al., Influence of thermal processing protocol upon the crystallization and photovoltaic performance of organic–inorganic lead trihalide perovskites, J. Phys. Chem. C 118 (2014) 17171–17177.
[7] Wanyi Nie et al., High-efficiency solution-processed perovskite solar cells with millimeter-scale grains, Science 347 (2015) 522–525.
[8] Yehao Deng et al., Air-stable, efficient mixed-cation perovskite solar cells with Cu electrode by scalable fabrication of active layer, Adv. Energy Mater. 6 (11) (2016), 1600372.
[9] Hsueh-Chung Liao et al., Enhanced efficiency of hot-cast large-area planar perovskite solar cells/modules having controlled chloride incorporation, Adv. Energy Mater. (2017) 1601660.
[10] Ashish Dubey et al., Strategic review on processing routes towards highly efficient perovskite solar cells, J. Mater. Chem. A 6 (2018) 2406–2431.
[11] Maria João Brites et al., Ultra-fast low-temperature crystallization of solar cell graded formamidinium-cesium mixed-cation lead mixed-halide perovskites using a reproducible microwave-based process, ACS Appl. Energy Mater. 23 (2019) 1844, https://doi.org/10.1021/acsaem.8b02005.
[12] David P. McMeekin et al., Science 351 (6269) (2016) 151–155.
[13] S.V. Egorov et al., Edge effect in microwave heating of conductive plates, J. Phys. D: Appl. Phys 39 (2006) 3036–3041.
[14] Md Ataul Mamun et al., Rapid and low temperature processing of mesoporous and nano-crystalline TiO_2 film using microwave irradiation, ACS Appl. Energy Mater. 1 (11) (2018) 6288–6294.
[15] Jin Sun, Wenlong Wang, Qinyan Yue, Review on microwave-matter interaction fundamentals and efficient microwave-associated heating strategies, Materials 9 (2016) 231.
[16] Satoshi Uchida et al., Flexible dye-sensitized solar cells by 28 GHz microwave irradiation, J. Photochem. Photobiol. A: Chem. 164 (2004) 93–96.
[17] N. Judy, Hart et al, Microwave processing of TiO_2 blocking layers for dye-sensitized solar cells, J. Sol-Gel Sci. Technol. 40 (2006) 45–54.
[18] Antonio De La Hoz, André Loupy, in: Microwaves in Organic Synthesis, John Wiley & Sons, New Jersey, 2013, p. 1.
[19] Keith Thompson et al., RF and Microwave Rapid Magnetic Induction Heating of Silicon Wafers in Advances in Microwave and Radio Frequency Processing, Springer, Berlin, 2006, p. 674.
[20] Qipeng Cao et al., Fast and controllable crystallization on perovskite films by microwave irradiation process, Appl. Mater. Interfaces 8 (12) (2016) 7854–7861.
[21] Buyoung Jung, Kangmin Kim, Woochul Kim, Microwave-assisted solvent vapor annealing to rapidly achieve enhanced performance of organic photovoltaics, J. Mater. Chem. A 2 (2014) 15175–15180.
[22] L. Ratke, P.W. Voorhees, Growth and Coarsening: Ostwald Ripening in Material Processing, Springer Verlag Berlin Heidelberg, New York, 2002.
[23] Antonio de la Hoz, Ángel Diaz-Ortiz, Andrés Moreno, Microwaves in organic synthesis. Thermal and non-thermal microwave Effects, Chem. Soc. Rev. 34 (2005) 164–178.